NASA Technical Memorandum 86776

NASA-TM-86776 19850025803

# Use of Hyperbolic Grid Generation Scheme in Simulating Supersonic Viscous Flow About Three-Dimensional Winged Configurations

Yehia M. Rizk, Joseph L. Steger and Denny S. Chaussee

July 1985

NASA
National Aeronautics and
Space Administration

NF00039

NASA Technical Memorandum 86776

# Use of Hyperbolic Grid Generation Scheme in Simulating Supersonic Viscous Flow About Three-Dimensional Winged Configurations

Yehia M. Rizk, Informatics General Corporation, Palo Alto, California
Joseph L. Steger
Denny S. Chausse, Ames Research Center, Moffett Field, California

July 1985

*N85-34116*

# USE OF A HYPERBOLIC GRID GENERATION SCHEME IN SIMULATING SUPERSONIC VISCOUS FLOW ABOUT THREE-DIMENSIONAL WINGED CONFIGURATIONS

Yehia M. Rizk

Informatics General Corp., Palo Alto, California, 94303.

Joseph L. Steger and Denny S. Chaussee

NASA Ames Research Center, Moffett Field, California, 94035.

## Abstract

The objectives of this paper is 1)to describe an efficient numerical mesh generation technique capable of creating single grids around complex winged configurations, 2)use the above grid generation scheme to simulate the flow field around a realistic three dimensional configuration by solving the Reynolds averaged Navier-Stokes equations using a time dependent implicit procedure. Numerical results are presented for the flow around the complete configuration of the shuttle orbiter and a canard projectile at supersonic Mach numbers and zero angle of attack.

## Introduction

The present paper describes a numerical mesh generation technique (Ref. [1]) and an implicit finite-difference procedure (Refs. [2,3]) for simulating viscous flow about low- aspect-ratio wing body configurations using a single grid strategy. Meshes are generated for complex three-dimensional winged configurations using equations of mesh line orthogonality and cell volume which form a hyperbolic partial differential equation set. The grid generation equations are readily solved in the computational domain by marching outward from the body surface. In supersonic flow, the three-dimensional Reynolds-averaged Navier Stokes equations are efficiently solved by segmenting the computational domain into multiple regions([3]).This is possible because the outflow boundary of each segment can be located in supersonic areas to avoid upstream influence between two contiguous regions.

The numerical procedures have been used to compute the viscous high Reynolds number flow around a complete configuration of the shuttle orbiter (including the canopy, wing, OMS pods and vertical tail) and a canard projectile at supersonic Mach numbers and zero angle of attack. In the following sections, we briefly describe the grid generation procedure, the flow simulation procedure, and the computed results.

## Numerical Grid Generation Procedure

Although, there are various grid generation techniques available, (see e.g. [4]), the hyperbolic grid generation method ([1],[5]) was selected in the present applications because it has several desirable features. With the hyperbolic grid generation

method, the user is able to specify an arbitrary surface point distribution, and the numerically generated grid is orthogonal or is as close to being orthogonal as possible. The hyperbolic grid generation procedure is also efficient in terms of computer time and memory.

## Grid Generation Equations

Body-fitted curvilinear coordinates of $\xi = \xi$ (x, y, z), $\eta = \eta$ (x, y, z), and $\varsigma = \varsigma$ (x, y, z), where $\varsigma$ is the outward direction, are sought to simplify the application of finite-difference viscous flow field simulation procedures. Following Ref. [1], two orthogonality relations and a cell volume constraint are used as grid generation equations to provide x, y and z in terms of $\xi$, $\eta$ and $\varsigma$. The resulting equations are:

$$x_\xi x_\varsigma + y_\xi y_\varsigma + z_\xi z_\varsigma = 0 \tag{1a}$$

$$x_\eta x_\varsigma + y_\eta y_\varsigma + z_\eta z_\varsigma = 0 \tag{1b}$$

$$x_\xi y_\eta z_\varsigma + x_\varsigma y_\xi z_\eta + x_\eta y_\varsigma z_\xi - x_\xi y_\varsigma z_\eta - x_\eta y_\xi z_\varsigma - x_\varsigma y_\eta z_\xi = \Delta V \tag{1c}$$

or with $\vec{r}$ defined as $(x, y, z)^t$

$$\vec{r}_\xi \cdot \vec{r}_\varsigma = 0 \tag{2a}$$

$$\vec{r}_\eta \cdot \vec{r}_\varsigma = 0 \tag{2b}$$

$$\left| \frac{\partial(x, y, z)}{\partial(\xi, \eta, \varsigma)} \right| = J^{-1} = \Delta V \tag{2c}$$

The first two equations represent orthogonality relations between $\xi$ and $\varsigma$ lines and between $\eta$ and $\varsigma$ lines, whereas the last equation is the cell volume or the finite Jacobian constraint.

## Numerical Solution Algorithm

The nonlinear system of grid generation equations given by Eqs. (1) are linearized about a known state $r_0$, and are solved using a noniterative implicit finite-difference scheme. An unconditionally stable implicit scheme is chosen so that the marching step size in $\varsigma$ can be arbitrarily selected based only on considerations of accurately generating the grid. An iterative solution of the nonlinear grid generation equations is avoided by expanding the equations about the previous marching step. As a consequence, the resulting equations are solved with the nearby known state $_0$ taken from the previous $\varsigma$ step.

Let $\Delta \xi = \Delta \eta = \Delta \varsigma = 1$ such that $\xi = j - 1, \eta = k - 1$, and $\varsigma = l - 1$. Central spatial differencing of Equations (1) in $\xi$ and $\eta$ with two-point backward implicit differencing in $\varsigma$ leads to

$$A_l \delta_\xi (\vec{r}_{l+1} - \vec{r}_l) + B_l \delta_\eta (\vec{r}_{l+1} - \vec{r}_l) + C_l \nabla_\varsigma \vec{r}_{l+1} = \vec{g}_{l+1} \tag{3}$$

where $I$ is the identity matrix, and $A_l, B_l$ and $C_l$ are $3 \times 3$ coefficient matrices that are formed from the local linearization of Eqn. (2). The vector $\vec{g}_{l+1}$ contains the user specified cell volumes

2

$$\vec{g}_{l+1} = \begin{pmatrix} 0 \\ 0 \\ \Delta V_{l+1} \end{pmatrix}$$

The central difference operators used in $\xi$ and $\eta$ are given by

$$\delta_\xi \vec{r}_j = \frac{\vec{r}_{j+1} - \vec{r}_{j-1}}{2}, \quad \delta_\eta \vec{r}_k = \frac{\vec{r}_{k+1} - \vec{r}_{k-1}}{2}$$

whereas the backward differencing used in $\varsigma$ is represented as

$$\nabla_\varsigma \vec{r}_{l+1} = \vec{r}_{l+1} - \vec{r}_l$$

To reduce the inversion cost, the difference equations are multiplied through by $C_l^{-1}$ and are approximately factored as

$$(I + C_l^{-1} B_l \delta_\eta)(I + C_l^{-1} A_l \delta_\xi)(\vec{r}_{l+1} - \vec{r}_l) = C_l^{-1} \vec{g}_{l+1} \qquad (4)$$

so that $\vec{r}_{l+1}$ is obtained by solving sequences of one–dimensional–like block tridiagonal systems

$$(I + C_l^{-1} B_l \delta_\eta) \vec{g}^{..}_{l+1} = C_l^{-1} \vec{g}_{l+1} \qquad (5a)$$

$$(I + C_l^{-1} A_l \delta_\xi) \nabla_\varsigma \vec{r}_{l+1} = \vec{g}^{..}_{l+1} \qquad (5b)$$

$$\vec{r}_{l+1} = \vec{r}_l + \nabla_\varsigma \vec{r}_{l+1} \qquad (5c)$$

In practice numerical dissipation terms are added in the $\xi$ and $\eta$ directions and for body shapes that have concavity, super implicitness is built into the algorithm following Ref. [6].

**Initial and Boundary Conditions**

The body surface is mapped to the bottom of the computational cube and the grid is obtained by marching outward from the body surface. The surface grid can be arbitrarly specifed by the user. For relatively simple body shapes, the user can generate an orthogonal grid along the body surface. This process assures that the resulting grid will be nearly orthogonal in all directions. For complicated configurations, however, the surface grid is generated along cross sections of constant axial distance. Depending on the body shape, the $\xi$ and $\eta$ lines can be far from being orthogonal. However, this does not introduce any inconsistency because the orthogonality between the $\xi$ and $\eta$ is not enforced in the grid generation procedure.

Boundary conditions in the $\xi$ and $\eta$ directions at each marching step are needed to create the grid. Periodicity is always used in the $\eta$ (circumferential) direction. A stable boundary condition procedure is needed at $\xi = 0$ and $\xi = \xi_{max}$ for creating "O-O" meshes around closed bodies(Fig. (1a)) and "C-O" or "H-O" meshes around

3

open bodies(Fig. (1b, 1c)) As shown in Ref. [1], the eigenvalues of either $C_l^{-1}A$ or $C_l^{-1}B$ are of the form $(\sigma, 0, -\sigma)$ where $\sigma$ is real. Consequently, two stable boundary procedures have been used: 1) specify one combination of the dependent variables and use one sided differencing for the two remaining governing equations at the boundary, or 2)specify two combinations of the dependent variables and use one sided differencing for a third governing equation at the boundary. The first approach is used at a boundary surface (e.g. $\xi = \xi_{max}$ in Figs. (1b, 1c)) whereas the second approach is used at an axis (e.g. $\xi = 0$ in Figs. (1a, 1b)).

Since, the grid is obtained by marching outward from the body, an exact location for the outer boundary can not be prescribed. Nevertheless, an approximate location for the outer boundary can be specified through proper selection of the cell volumes used in Eqn. (1c).

## FLOW SIMULATION PROCEDURE

The main objective of the present work is to demonstrate an efficient numerical procedure for computing three-dimensional viscous flow over winged configurations (e.g., the shuttle orbiter) at supersonic free-stream Mach numbers. Although the flow is predominantly supersonic, some sections of the geometry generate local regions of embedded subsonic flow and/or axial separation. In such regions, the flow equations are elliptic, precluding the use of the more efficient space-marching techniques such as the parabolized Navier-Stokes (PNS) codes (e.g. Ref. [7]). Instead, a time-dependent continuation procedure is used to find the steady-state solution of the three-dimensional conservation-law form of the Reynolds-averaged Navier-Stokes equations with the thin layer approximation.

The numerical procedure employs the vectorized Beam-Warming, approximate factorization, finite-difference scheme as presented in Refs. [2,3]. The algorithm is implicit, non-iterative and uses second or fourth-order accurate central-differencing in the spatial directions. A generalized coordinate transformation is employed to map the three- dimensional region between the body and the outer boundary into a cubical computational domain. The grid points are clustered in the direction normal to the body surface in such a manner as to adequately resolve both the viscous and the inviscid regions. The algebraic model of Ref. [8] is used for turbulent computations. The bow shock can either be fitted or captured while internal discontinuities are always captured. Calculations are performed using bilateral symmetry with the computational domain extending from the windward to the leeward side.

In order to facilitate the solution of the Navier-Stokes equations around complex bodies, a segmentation procedure in which the flow field is divided into multiple regions is used. The boundary between two adjacent regions is carefully located in areas where the outer inviscid flow is supersonic and the boundary layer is attached. This ensures the absence of any upstream influence between different regions and hence eliminates the otherwise costly interfacing between neighboring regions. Segmentation has been implemented in the current application to reduce the size of

4

the time dependent computational domain. Moreover, segmentation allows the use of the more efficient space marching procedure in any region not containing an embedded subsonic or axially separated flow.

## RESULTS

The current numerical technique has been used to simulate the flow field around the entire configuration of the shuttle orbiter and a simple projectile with a canard.

**Shuttle Orbiter**

The supersonic viscous flow about the shuttle orbiter has been computed using the four computational segments or regions shown in Fig. (2). The bow shock segment, Region I, is treated as a typical blunt body problem with supersonic outflow and is solved using a time-relaxation code. Region II is centered about the canopy and is also solved with the time dependent code because the canopy shock induces a small region of subsonic flow. Region III is purely supersonic and could be solved by space marching, but for ease of application the more robust time dependent code was again utilized. Finally, Region IV containing the wing, the OMS pods, and vertical tail has embedded regions of subsonic flow as well as regions of axial separation and must be solved using the time dependent code. In Region IV it is particularly important that the generated mesh be body normal, both in the cross-sectional and axial planes in order to resolve the viscous flow over different components of the orbiter which are inclined at relatively steep angles to the fuselage.

The hyperbolic grid generation procedure was used to generate the grids in Regions II, III and IV, whereas an algebraic procedure was used for the simple nose geometry. Figure (3) indicates the $25 \times 123 \times 29$ grid generated for Region IV in which there are 25 points in the axial direction, 123 points in the circumferential direction, and 29 points in the normal direction. Projections of either $\eta = constant$ or onto $\xi = constant$ grid planes onto either $y = constant$ or $x = constant$ planes are used to illustrate the grid. Figure (3a), for example, shows a segment of the grid near the beginning of the vertical tail in the $\eta = constant$ leeward plane of symmetry. Figures (3b) to (3d) show various $\xi = constant$ grid planes projected into the $y - z$ plane. It is seen that the grid lines are normal to the body surface.

The pressure contours in a cross section containing the wing, OMS pods and vertical tail are shown in Fig. (4). A side view of the simulated oil flow (i.e. limiting streamlines) at the body surface are shown in Fig. (5). It is seen that there is an area of axially separated flow upstream of the vertical tail and the OMS pods. The location of the separation line coincides with a line along which the limiting streamlines coalesce while the reattachment line coincides with a line at which the limiting streamlines diverge.

The computations were performed on the CRAY-XMP-12 with one central processor and two millions words of memory. The code is vectorized and the metrics are not stored but are computed when needed. The computer time required per

5

grid point is 0.00012 sec per iteration.

## Canard Projectile

The numerical procedure was also used to compute the flowfield around a projectile with a canard at a Mach number of 4 and zero angle of attack. The geometry (Fig. (6)) consists of an 8 degree blunted cone followed by a cylinder. A canard protrudes from the cylinder at a plane 90 degrees from the pitch plane of symmetry. The hyperbolic grid generation scheme was used to create the three- dimensional mesh required for the viscous computations. Various views of the grid are depicted in Fig. (7). It is seen that the grid is body normal in both the streamwise and meridional directions. It is also seen that a clustering is employed in the outward direction in order to resolve the viscous effects near the body surface. In addition, a simple streamwise clustering is introduced to adequately resolve the flow features in the wake of the canard.

In generating the grid, the cell volumes were specified such that the outer boundary is nearly conical with a half cone angle of approximately 20 degrees. This assures that the bow shock is located well inside the outer boundary because the shock angle corresponding to an 8 degree cone at Mach number 4 is about 18 degrees.

The above mesh was then partitioned into three longitudinal segments. The first segment contains the spherical nose. The second segment contains the conical section and the front portion of the canard. The third segment contains the back end of the canard and the cylindrical portion. An axisymmetric blunt body code was used to compute the flow field in the first segment. The flow field in the second and third segments were obtained using the time relaxation procedure of Ref. [3]. Because the body is at zero angle of attack, the computational domain was confined to the region between $\phi = 0$ and $\phi = 90$ degrees. The results of the calculations in the second segment revealed the absence of any embedded subsonic flow bubbles or axially separated flow regions. This means that a PNS code could have been utilized in this region.

The results of the computations in the third segment are shown in Figs. (8-12). The Mach contours in the $\phi = 90$ degrees symmetry plane (canard plane) are shown in Fig. (8). It is seen that there is a relatively large subsonic bubble residing in the canard wake. The velocity vectors in the canard plane are shown in Fig. (9). The regions of axial flow separation and reattachment are clearly visible from the corresponding limiting streamlines depicted in Fig. (10). The pressure contours and velocity vectors in a streamwise stations corresponding to the canard full extent and in the cylindrical portion are shown in Figs. (11, 12) and (13, 14) respectively. The above computations were obtained using 88125 grid points on the CRAY-XMP-12. The computer time per time step is approximately 13 seconds. A total of 800 iterations were required for convergence.

## SUMMARY

The present paper described a numerical mesh generation technique to be used

6

with an implicit finite-difference method for simulating viscous supersonic flow about low-aspect-ratio wing body configurations using a single grid strategy. The computational domain was segmented into multiple regions, with borders located in supersonic areas to avoid the otherwise costly interfacing procedure between adjacent segments. The numerical procedure has been successfully applied to calculate the turbulent flow around the shuttle orbiter and a canard projectile at supersonic free-stream Mach number.

## REFERENCES

1)Steger, J.L., and Rizk, Y.M.,"Generation of Three Dimensional Body Fitted Coordinates Using Hyperbolic Partial Differential Equations." NASA TM 86753, June, 1985 (also AFWAL-TR 83-3129, Feb., 1984)

2) Pulliam, T.H., and Steger, J.L, "On Implicit Finite-Difference Simulations of Three Dimensional Flow," AIAA Paper No. 78-10, Huntsville, Ala., Jan., 1978.

3) Rizk, Y.M., and Ben-shmuel, S.,"Computation of the Viscous Flow Around the Shuttle Orbiter at Low Supersonic Speeds.", AIAA Paper 85-0168, Reno, Nevada, Jan., 1985.

4)Thompson, J.F.,"Numerical Grid Generation", Proceedings of a Symposium on the Numerical Generation of Curvilinear Coordinate Systems and Their Use in the Numerical Solution of Partial Differential Equations.1982, Nashville, Tennesee.

5)Steger, J.L., and Chaussee, D.S.,"Generation of Body Fitted Coordinate Using Hyperbolic Partial Differential Equations," SIAM Journal Sci. Stat. Comput., Vol. 1, No. 4, Dec. 1980, pp. 431-437

6)Kinsey, D.W., and Barth, T.J. "Description of a Hyperbolic Grid Generation Procedure for Arbitrary Two-Dimensional Bodies", AFWAL Technical Memorandum No.84-191-FIMM (July, 1984)

7) Schiff, L.B., and Steger, J.L., " Numerical Simulation of Steady Supersonic Viscous Flow,"AIAA Journal, Vol.18, Dec. 1980., pp 1421-1430.

8) Baldwin, B.S., and Lomax, H.,"Thin Layer Approximation and Algebriac Model for Separated Turbulent Flows,"AIAA Paper No.78-257, Huntsville, Ala, 1978.

BOUNDARY SURFACE
$\xi = \xi_{max}$

$\zeta$

AXIS
$\xi = 0$

$\xi$

$\eta$

AXIS
$\xi = \xi_{max}$

$\zeta$

$\xi$

$\eta$

AXIS
$\xi = 0$

O–O MESH (SPHERICAL LIKE)     C–O MESH (SEMI-SPHERICAL)
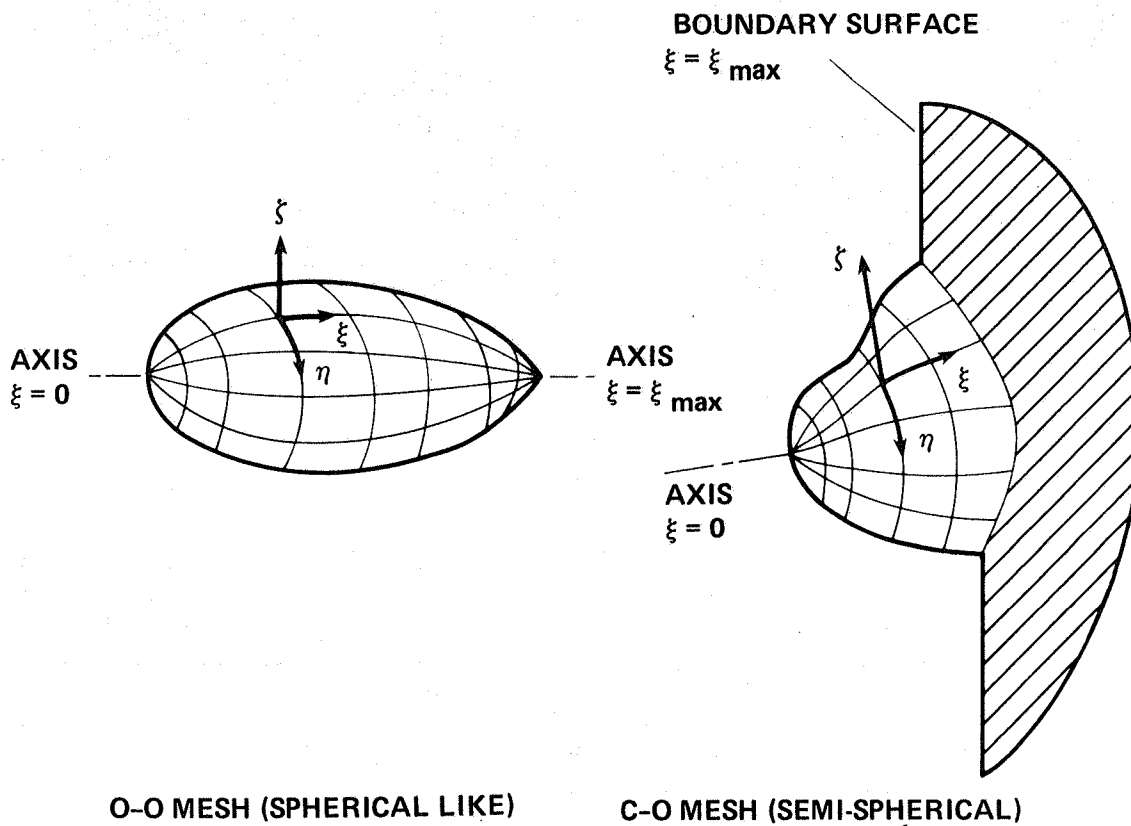
Fig. 1 Mesh topologies around closed and open
bodies.

BOUNDARY SURFACE
$\xi = \xi_{max}$

BOUNDARY SURFACE
$\xi = 0$

$\zeta$

$\xi$

$\eta$

H-O MESH (CYLINDRICAL LIKE)

Fig. 1 continued.



REGION I  REGION II  REGION III  REGION IV
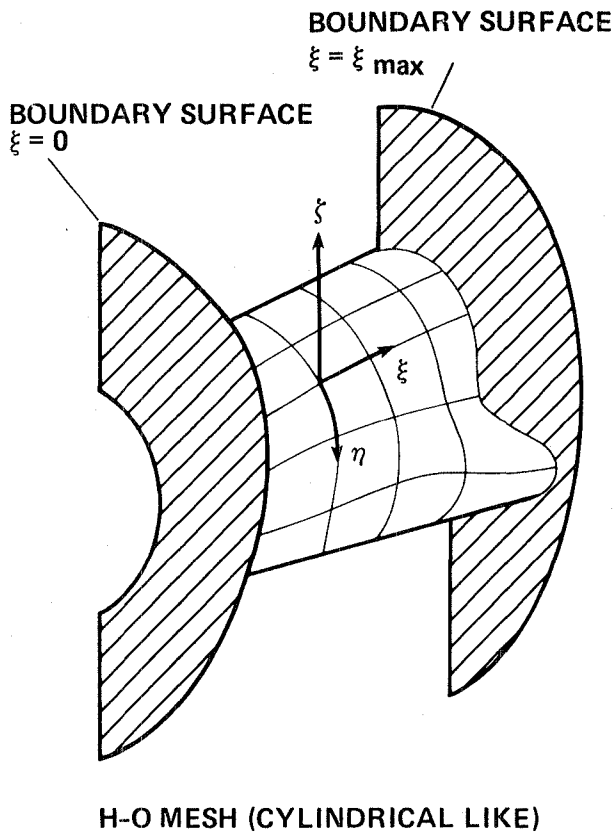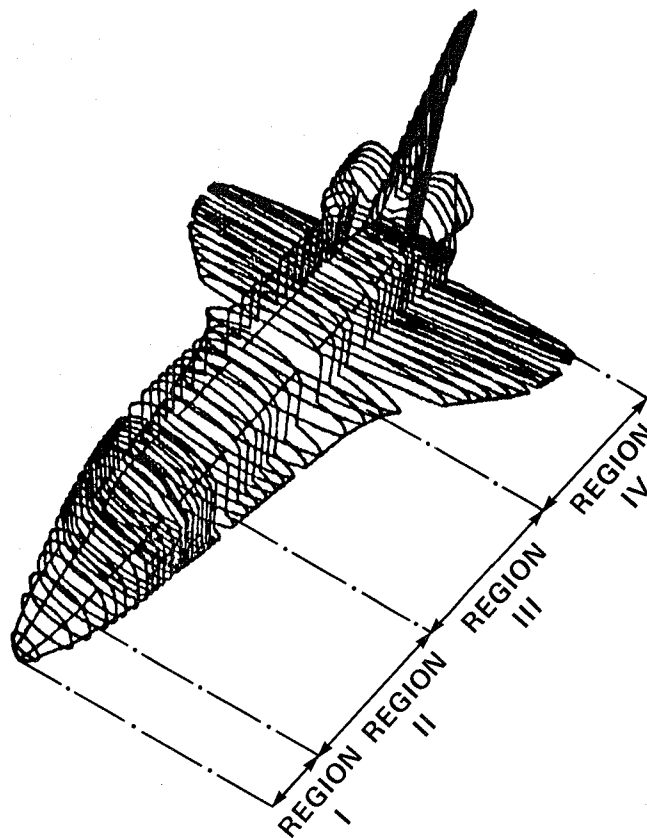
Fig. 2 Flow regions around the shuttle orbiter.
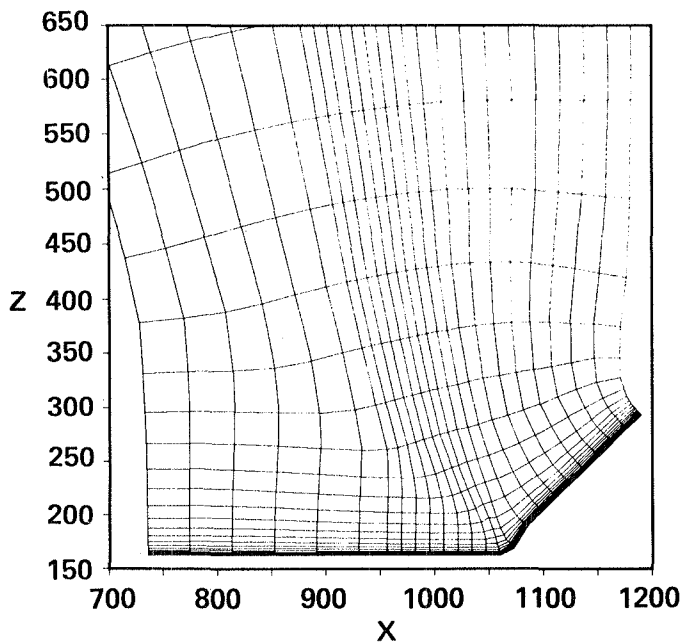


Fig. 3a Grid in the leeward plane of symmetry.
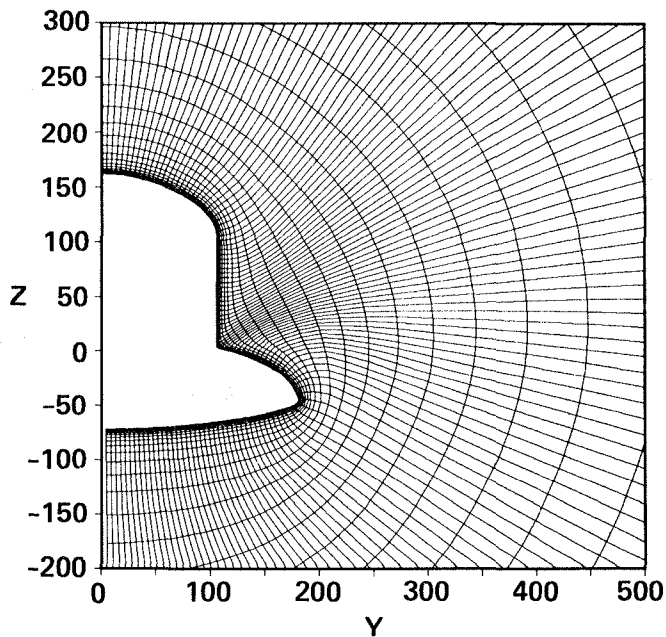


Fig. 3b Projection of the grid on an axis normal plane containing the strake.

9
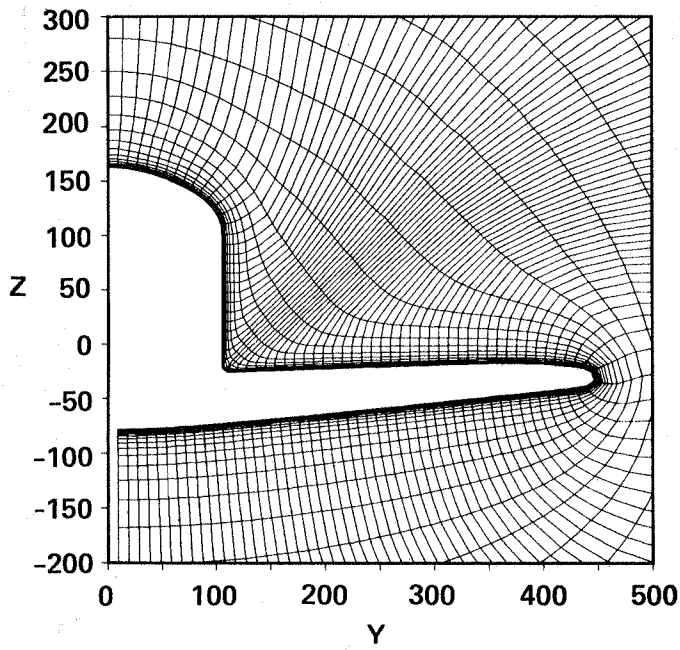
Fig. 3c Projection of the grid on an axis normal plane containing the wing.
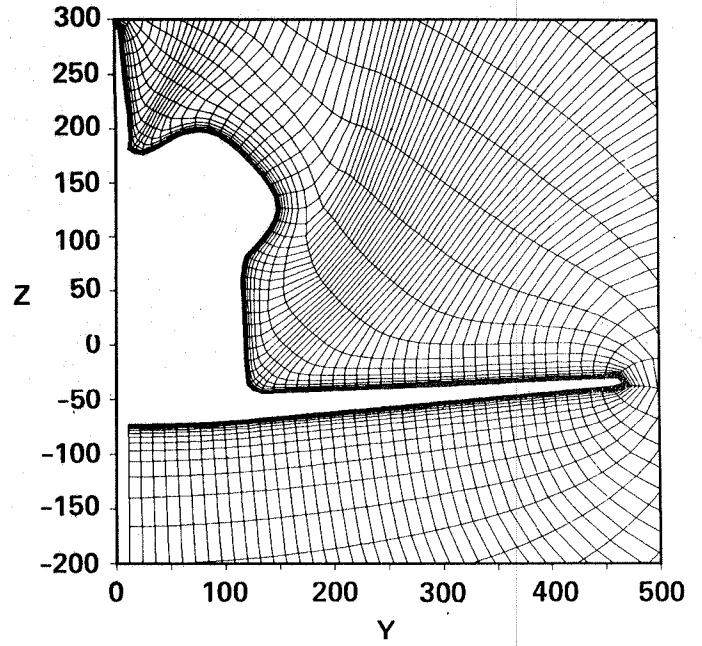


Fig. 3d Projection of the grid on an axis normal plane containing the wing, OMS pods and vertical tail.
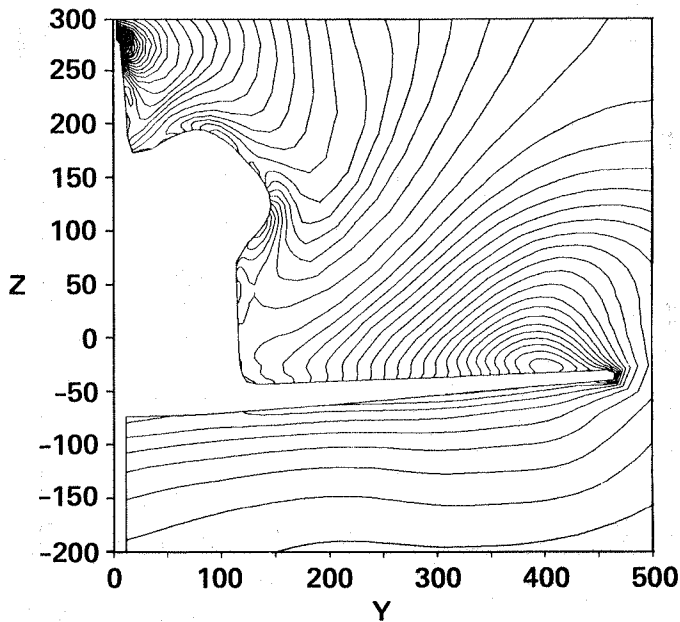


Fig. 4 Pressure contours in a cross section near the end of region IV.
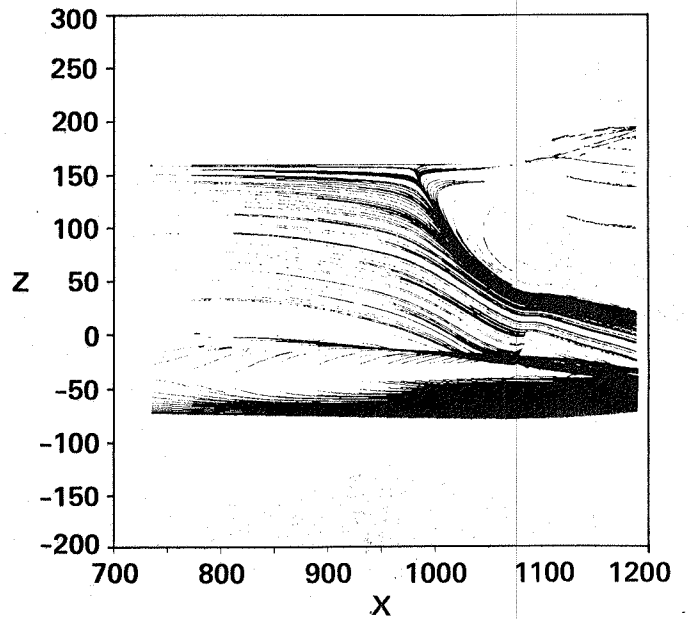


Fig. 5 Side view of the oil flow (limiting streamlines) in region IV.

10
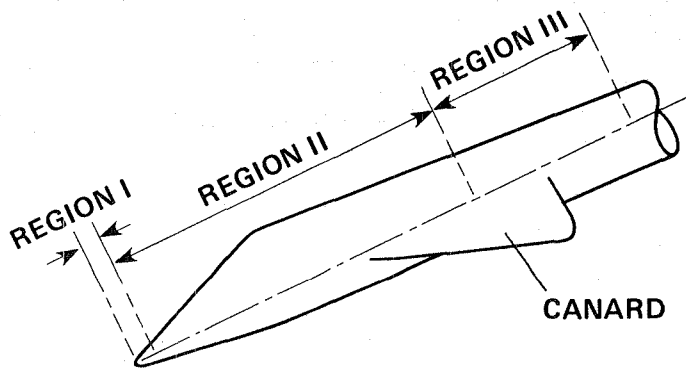
Fig. 6 Flow regions around a projectile with a canard.
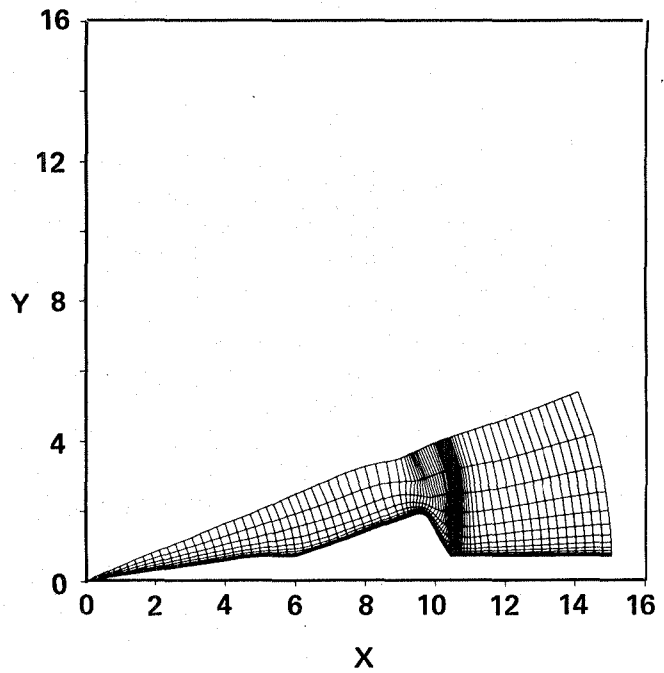


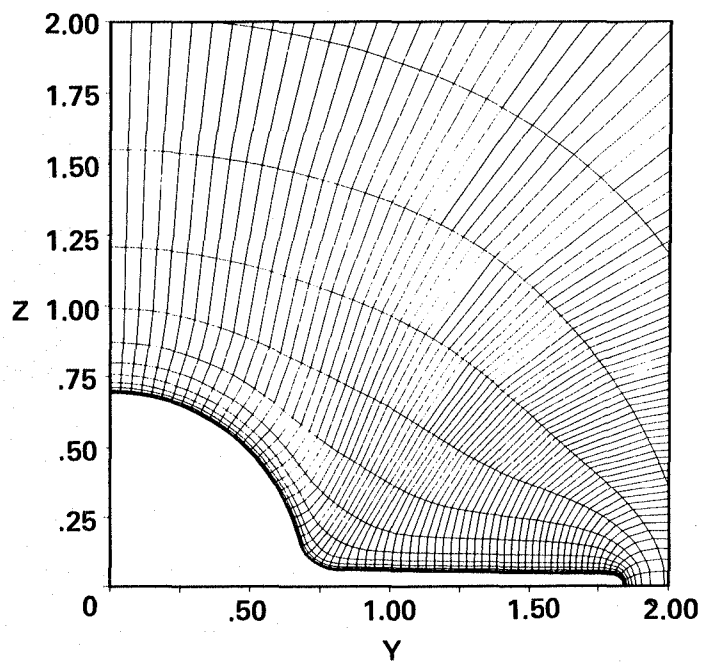Fig. 7a Grid in the canard plane of symmetry.
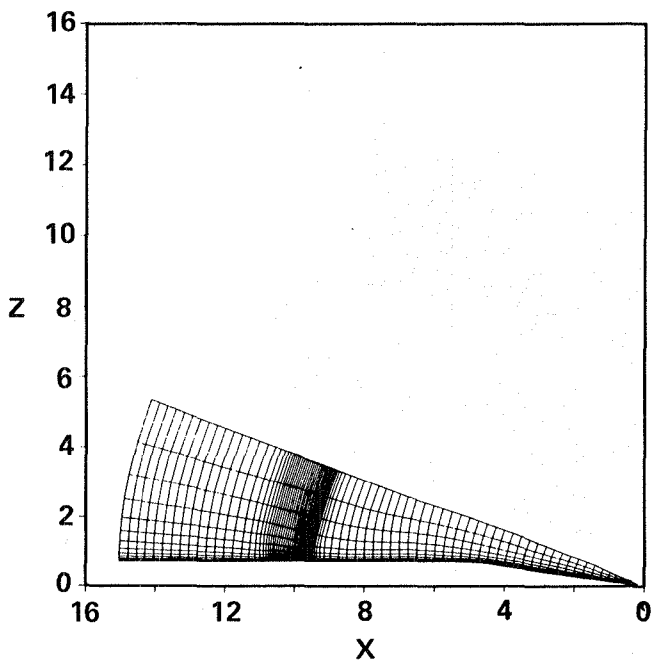


Fig. 7b Grid in the leeward plane of symmetry.



Fig. 7c Grid in a cross section containing the canard.
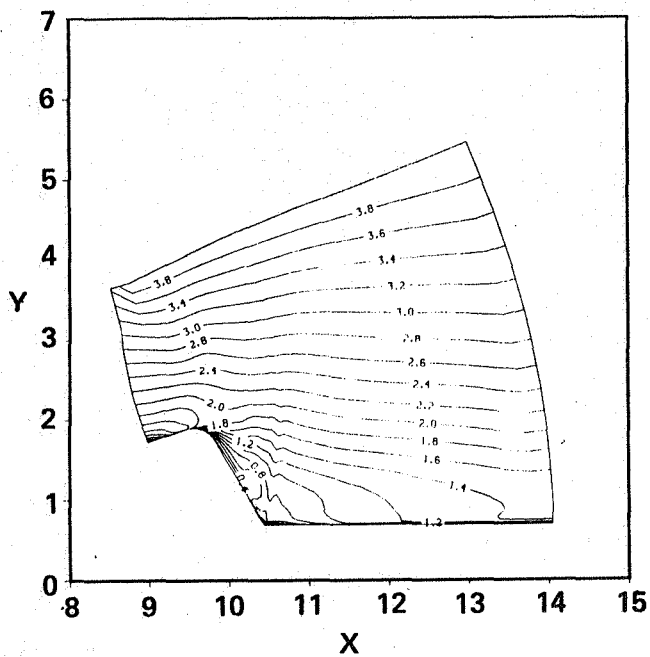
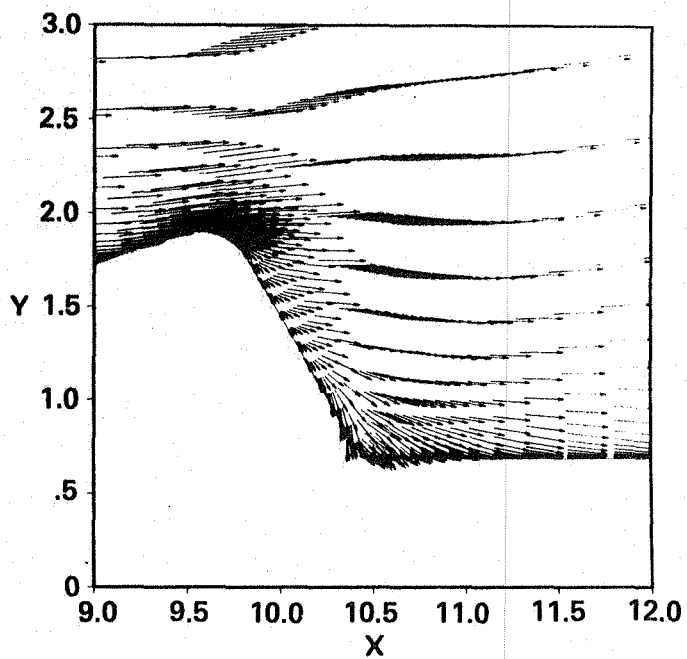Fig. 8 Mach number contours in the canard symmetry plane.



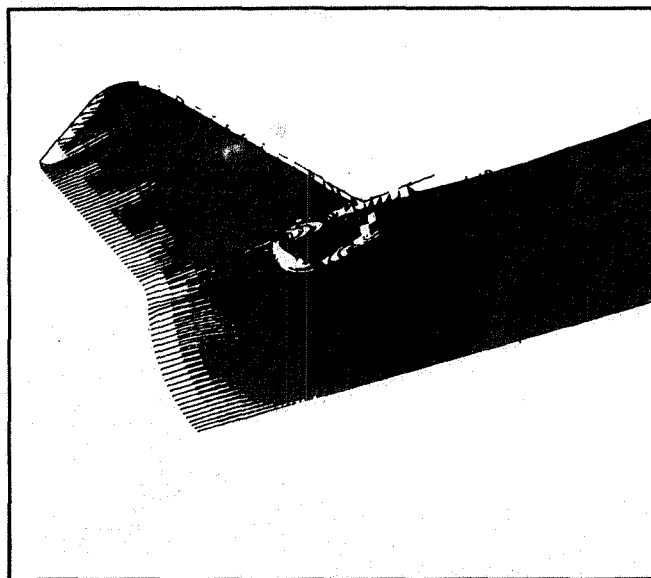Fig. 9 Velocity vectors in the canard plane of symmetry.



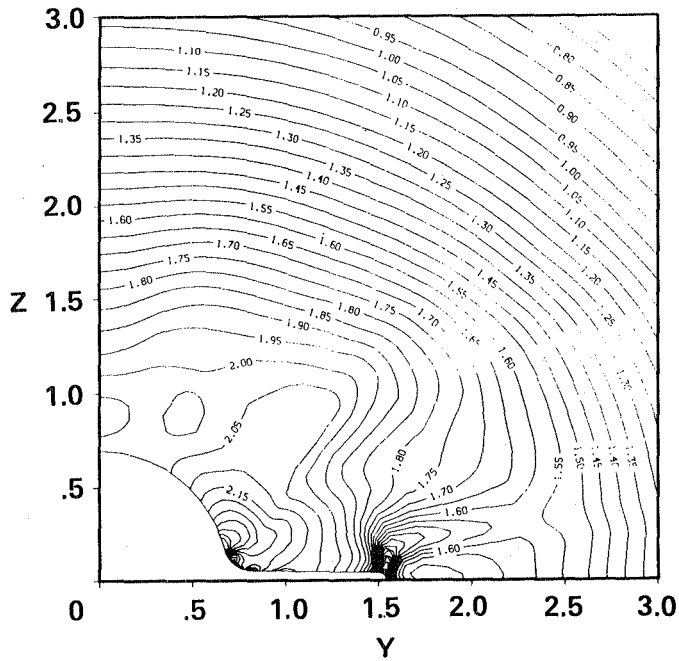Fig. 10 Limiting streamlines (simulated oil flow) in the canard region.

Fig. 11 Pressure contours in a cross section corresponding to the full extent of the canard.
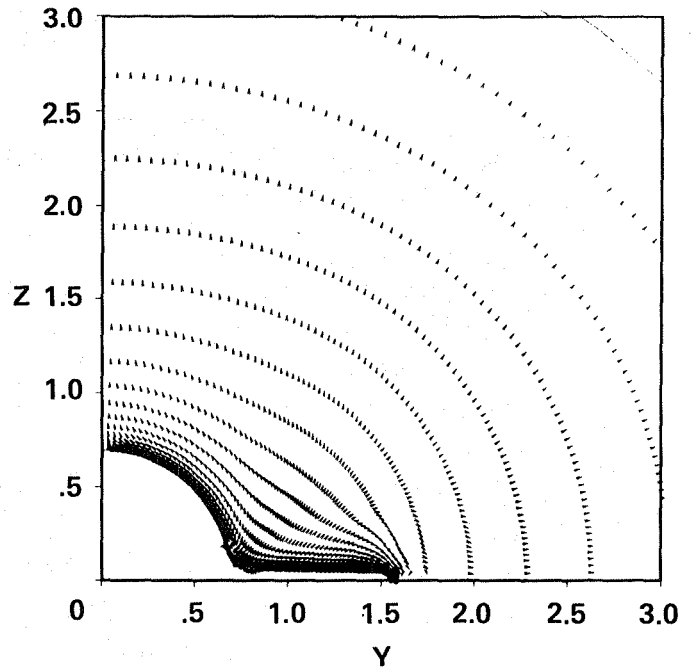


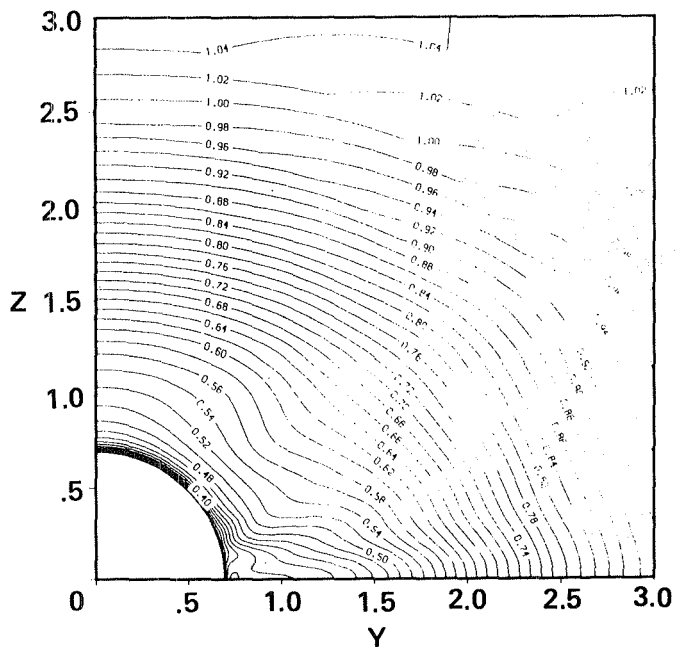Fig. 12 Velocity vectors in a cross section corresponding to the full extent of the canard.



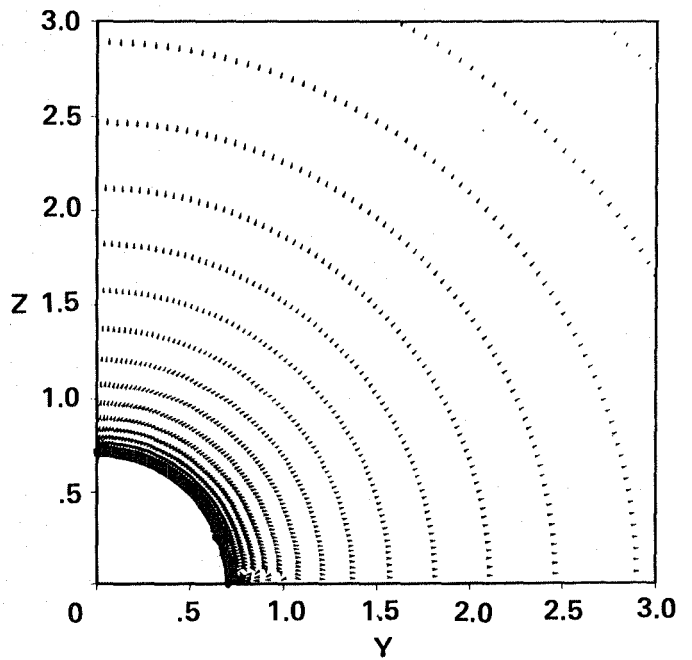Fig. 13 Pressure contours in a cross section in the wake of the canard.



Fig. 14 Velocity vectors in a cross section in the wake of the canard.

| 1. Report No. NASA TM-86776 | 2. Government Accession No. | 3. Recipient's Catalog No. |
|---|---|---|
| 4. Title and Subtitle<br>USE OF A HYPERBOLIC GRID GENERATION SCHEME IN SIMULATING SUPERSONIC VISCOUS FLOW ABOUT THREE-DIMENSIONAL WINGED CONFIGURATION | | 5. Report Date<br>July 1985 |
| | | 6. Performing Organization Code |
| 7. Author(s) Yehia M. Rizk (Informatics General Corp., Palo Alto, Calif.), Joseph L. Steger, and Dennis S. Chaussee | | 8. Performing Organization Report No.<br>85344 |
| | | 10. Work Unit No. |
| 9. Performing Organization Name and Address<br>Ames Research Center<br>Moffett Field, CA 94035 | | 11. Contract or Grant No. |
| | | 13. Type of Report and Period Covered<br>Technical Memorandum |
| 12. Sponsoring Agency Name and Address<br>National Aeronautics and Space Administration<br>Washington, DC 20546 | | 14. Sponsoring Agency Code<br>505-31-01 |

15. Supplementary Notes

Point of contact: Yehia M. Rizk, Ames Research Center, MS N202A-14, Moffett Field, CA 94035    (415) 694-6329 or FTS 464-6329

16. Abstract

    The present paper describes a numerical mesh generation technique to be used with an implicit finite difference method for simulating viscous supersonic flow about low-aspect-ratio wing body configurations using a single grid strategy. The computational domain is segmented into multiple regions, with borders located in supersonic areas to avoid the otherwise costly interfacing procedure between adjacent segments. The numerical procedure is applied to calculate the turbulent flow around the shuttle orbiter and a canard projectile at supersonic free stream Mach number.

| 17. Key Words (Suggested by Author(s))<br>Computational fluid dynamics<br>Grid generation<br>Three-dimensional viscous flow | 18. Distribution Statement<br>Unlimited<br><br>Subject category: 02 | | |
|---|---|---|---|
| 19. Security Classif. (of this report)<br>Unclassified | 20. Security Classif. (of this page)<br>Unclassified | 21. No. of Pages<br>15 | 22. Price*<br>A02 |

**End of Document**